Malaysian Journal of Chemistry, 2023, Vol. 25(3), 286-294
(Special Issue: *3rd IKMPB Online Symposium 2023 - Innovation in Chemistry Towards Sustainable Development*)

Preparation and Chracterization of Chitosan-Silver Nitrate (Cs-$AgNO_3$) Nanoparticles as Non-Woven Fabrics for Medical Applications

Juliana Sapik and Siti Amira Othman*
Faculty of Applied Sciences and Technology, University Tun Hussein Onn Malaysia
84600 Pagoh, Johor, Malaysia
*Corresponding author (e-mail: sitiamira@uthm.edu.my)

Some of the commercial wound dressings lack antibacterial properties and do not contribute to fastening the wound-healing process. This study was conducted to produce non-woven wound dressing based on chitosan (Cs) and silver nitrate ($AgNO_3$). A solution of wound dressing from pure chitosan and the combination of chitosan and silver nitrate (Cs-$AgNO_3$) with different concentrations of silver nitrate was prepared. Surface morphology and physical and chemical properties of pure chitosan and Cs-$AgNO_3$ nanoparticles were characterized using Field Emission Scanning Electron Microscopy (FESEM), Ultraviolet-Visible (UV-Vis) spectroscopy, and Fourier Transform Infrared (FTIR) spectroscopy. The results indicate the presence of an absorption peak at 286 nm and functional groups of amine, hydroxyl, and carbonyl in the sample solutions. The bundle shape image corresponds to pure chitosan, while the spherical shapes of particles belong to $AgNO_3$.The combination of Cs-$AgNO_3$ demonstrates promising properties as a future wound dressing for medical applications.

Keywords: Chitosan; silver nitrate; medical; wound dressing; woven fabrics

Received: December 2022 ; Accepted: April 2023

Non-woven fabric is widely used in medical textiles, especially as a wound dressing. which is one of the rapidly growing technical textiles of the textile industry worldwide [1]. An ideal wound dressing must have the following properties: being non-allergenic and nontoxic, keeping a moist environment, allowing gas exchange, absorbing wound exudate, and protecting the wound against microbial growth [2]. Chitosan is a non-toxic, biocompatible, and biodegradable polymer widely derived from the exoskeleton of insects and shells of crustaceans. It is used in many biomedical applications, such as drug delivery, cell delivery systems, orthopedics, wound healing, ophthalmology, and bone healing [3]. Chitosan also has some unique properties, like inhibiting the growth of a wide variety of bacteria and fungi, showing broad spectra of antibacterial activity, and possessing a high killing rate and low toxicity toward mammalian cells [4-6]. Due to the promising properties of chitosan, it is utilized in the textile industry, particularly in medical textiles. Silver has been extensively studied as an antimicrobial agent, primarily in the treatment of serious wounds [7]. It also has been used in clinical testing as an antimicrobial for over a century. Moreover, silver nitrate is a common anti-microbial used in the handling of chronic wounds. Silver nanoparticle (AgNPs) is one of the most famous nano-products for medical purposes, due to their antimicrobial activity. The properties of nanoparticles, such as the small size, provide a bigger surface contact with the bacterial cell, an increased penetration, and an enhanced bacterial effect. Chitosan and silver nano-particles have exhibited healing properties individually. Therefore, their combination can demonstrate an enhancement in wound-healing activity [8].

The properties of an ideal wound dressing are providing a moist environment around the wound, allowing the diffusion of gases, minimizing the pain from the wound, and being biocompatible and elastic. Some commercial wound dressings do not exhibit suitable healing properties only covering the wound without stimulating the hemostasis [9]. Currently, there are budgetary constraints on public hospitals forcing them to discharge patients early. With the increasing number of patients, advanced care products and early treatment cannot be affordable for government hospitals and clinics due to budget problems. This will contribute to poor healthcare outcomes and the increasing number of amputations [10]. In addition, the material of wound dressing is expensive. Therefore, the material selection of wound dressing is vital to help budgetary constraints. At the same time, it can accelerate the healing process of the patient. There are a lot of commercial wound dressing materials available, however, there is a lack of full understanding of wound care management by some of them [11]. Nowadays, a vital scientific challenge is to search for new therapeutic agents capable of working against the resistance of bacterial strains [12].

†Paper presented at the 3rd IKMPB Online Symposium 2023 - Innovation in Chemistry Towards Sustainable Development

The significance of this study is to provide extra knowledge, especially for newcomers to the field of biomedical application. Not only that the production of finished non-woven fabric ($AgNO_3$-chitosan composite) will help the industry to produce biocompatible, biodegradable, and environmentally friendly due to the use of green methods during producing this antibacterial non-woven fabric. Furthermore, the time it takes for the wound to heal also can be shortened due to the properties of both chitosan and silver nanoparticles as antibacterial agents. The previous studies indicate that this finished non-woven fabric has great potential for use as a medical dressing material [28]. The process of producing nonwoven is simple, productive, versatile, and low-cost compared to that of other types of fabrics. This study also demonstrates the application of nanotechnology in medical care field offering many important advantages. The properties of Cs-$AgNO_3$ in this study indicate the novel characteristics of non-woven fabrics. Moreover, applying nanotechnology and incorporating knowledge of cellular and subcellular events occurring during the typical healing process, may lead to better therapeutic interventions in the future.

EXPERIMENTAL

Materials

In this study, chitosan flakes were utilized to produce the wound dressing. Besides, other materials that had been used in this experiment were acetic acid, silver nitrate, sodium hydroxide, and non-woven swab were used. All the materials, except for the non-woven fabric, were bought from Sigma-Aldrich.

Preparation of the Treated Non-Woven Wound Dressing

Six samples, including pure chitosan and chitosan loaded with different concentrations of silver nitrate, were used in this experiment. The process of preparation of treated non-woven wound dressing is illustrated in Figure 1. 3.0 g of chitosan flakes was dissolved in 2 wt.% acetic acid (300 ml). The solution containing chitosan and acetic acid was stirred and heated at 60 ^oC to dissolve the chitosan quickly. Next, the solution was filtered; and the undissolved particles were removed. The solution was filtered using filter paper and a conical flask. Then, the solution was put in the magnetic stirrer at a medium-level of speed. Afterward, NaOH was added periodically until the pH of the solution reached 10, measured using a pH meter. Then, six 100 ml beakers were prepared. Every beaker was labeled as pure chitosan, 0.4, 0.8, 1.2, 1.6, and 2.0 corresponding to the sample of pure chitosan (Cs), Cs-0.4 ml of $AgNO_3$, Cs-0.8.ml of $AgNO_3$, Cs-1.2 ml of $AgNO_3$, Cs-1.6 ml of $AgNO_3$, and Cs-2.0 ml of $AgNO_3$. Every beaker was filled with 50 mL of the solution. Silver nitrate was then added based on Table 1. Lastly, all the samples were filtered again to obtain a clear solution.

Table 1. Quantity of the $AgNO_3$ in the samples.

Labelled of Samples	Volume of $AgNO_3$ (ml)	Mass of $AgNO_3$ (mg)	Molarity of $AgNO_3$ (M)
$AgNO_3$	0.4	0.14	0.002
	0.8	0.54	0.004
	1.2	1.22	0.006
	1.6	2.17	0.008
	2.0	3.40	0.010

(a) (b) (c) (d) (e)

Figure 1. Process of samples preparation (a) Chitosan was dissolved in acetic acid solution, (b) The pH of the solution was measured, (c) Filtration of the sample solutions, (d) Non-woven swab was soaked using forceps, (e) Preparation of non-woven swab for the drying process.

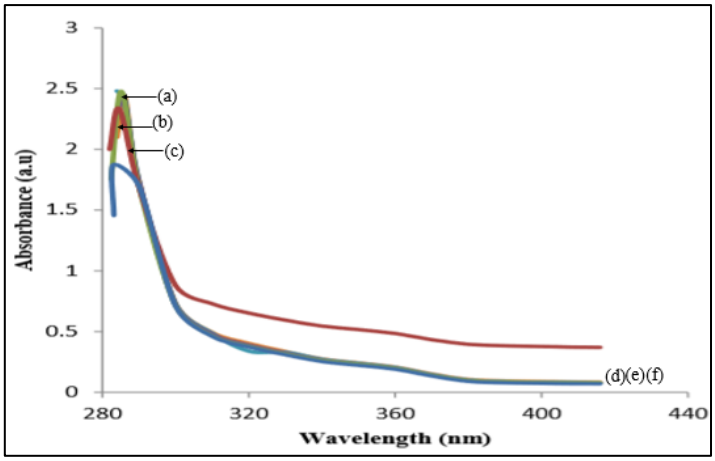

Figure 2. UV-Vis absorption spectra of the samples (a) Cs-1.2 ml of $AgNO_3$, (b) Cs, (c) Cs- 0.4 ml of $AgNO_3$, (d) Cs-0.8 ml of $AgNO_3$, (e) Cs-1.6 ml of $AgNO_3$, (f) Cs-2.0 ml of $AgNO_3$.

The filtered solution of the samples was characterized using Ultraviolet-visible (UV-Vis) spectrometer, Fourier Transform Infrared (FTIR) spectroscopy, and Field Emission Scanning Electron Microscope (FESEM). After that, the non-woven swabs were soaked with the filtered solution for 2 minutes. Next, the non-woven swabs were put in the crucible and dried in the oven for 4 min at 140°C. The dried non-woven fabrics were put in the labeled petri-dish sealed - with Parafilm. All the wound dressing samples were covered properly without direct exposure to the light to prevent the wound dressing from turning yellowish or brown color.

RESULTS AND DISCUSSION

The structures and chemical properties of the sample were identified using Field Emission Scanning Electron Microscope (FESEM), Ultraviolet-visible (UV-Vis) spectrometer and Fourier Transform Infrared Spectroscopy (FTIR).

Ultraviolet – visible Spectroscopic (UV-Vis) Analysis

Six samples of solution were analyzed using UV-Vis spectroscopy. The results (Figure 2) demonstrate that all samples exhibit an absorption band in the range of 283 nm to 286 nm. This range indicates typical Surface Plasmon Resonance (SPR) of conducting electrons from the surface of silver nanoparticles. However, the perfect absorption band for chitosan-AgNPs is in the range of 300–400 nm depending on the size, shape, and distribution of the samples. All five samples containing silver nitrate do not exhibit the perfect SPR band in the UV-Vis spectrum which can be problematic for the sample preparation. Not all sample solutions need to be prepared directly for UV-Vis characterization [13]. All the finished mixture samples must be waited for one hour or diluted with the acetic acid solution[1].

All the samples show the absorption spectrum assigned to the n-π^* transition. This is because the wavelength range of this transition is 200–700 nm [14]. Most of the absorption spectroscopy applications of organic compounds depend on this transition which has a very low absorptivity. Absorption of ultraviolet and visible radiation in organic molecules is restricted to a certain functional group, referred to as chromophores. The chromophores related to this range of wavelengths of the samples is carbonyl bond (C=O) with a wavelength of 280–290 nm. This band proves the absorption of Cs due to the chemical structure of chitosan ($C_6H_{11}O_4N$) enriched with the carbonyl, amine, and hydroxyl bonds. A sample of Cs-2.0 ml of $AgNO_3$ demonstrates the lowest absorption peak (Table 2) compared to other samples. This indicates that only a few molecules are absorbing the radiation. Thus, the total absorption of energy is less; and a lower peak of intensity is observed as a result [15].

The sample of Cs-1.2 ml of $AgNO_3$, exhibits the highest peak (Table 2). This confirms the presence of more molecules absorbing light at a given wavelength and the greater extent of light absorption which resulted in higher peak intensity of the absorption spectrum [15].

Fourier Transform Infrared Spectroscopy (FTIR)

FTIR studies changes in the vibrational and rotational movements of the molecules. It is frequently used to identify the presence or absence of functional groups which have specific vibrational frequencies (always referred to as wavenumber) [15]. FTIR has a range of wavenumber from 400 cm^{-1} to 4000 cm^{-1}. Wavenumbers give important structural knowledge about a compound. Even two same types of bonds in two different compounds may vibrate at different frequencies. Thus, there are no two compounds that can have the same infrared spectrum. To investigate the reduction process of silver nitrate with chitosan, FTIR characterization was conducted to study possible interactions responsible for the reduction of silver ions and stabilizing silver nanoparticles.

Table 2. Wavelengths and absorption peaks of UV-Vis spectroscopy.

Samples	Wavelength (λmax), nm	Absorption peak (a.u.)
Pure Chitosan (Cs)	286.0	2.44
Cs-0.4 ml of $AgNO_3$	286.0	2.43
Cs-0.8 ml of $AgNO_3$	286.0	2.41
Cs-1.2 ml of $AgNO_3$	285.2	2.48
Cs-1.6 ml of $AgNO_3$	284.6	2.33
Cs-2.0 ml of $AgNO_3$	283.0	1.88

Figure 3 illustrates the FTIR spectrum of the samples in the wavenumber region 450–4000 cm^{-1}. It can be seen from Figure 3, the samples of Cs-1.6 ml of $AgNO_3$ and Cs-2.0 ml of $AgNO_3$ have clear fluctuations in the percentage of transmittance (T.%). This shows that these samples have many rhythmical changes in the dipole moment of the molecule absorbing infrared radiations compared to that of other samples. This shows that these two samples were recognized as infrared active while the remaining samples, especially pure chitosan, were recognized as infrared inactive having weak dipole due to a lack of various changes in the absorption bands [15]. All the samples have strong absorption at the wavenumber around 3400 cm^{-1}. At this range of wavenumber, the functional group of alcohol (O-H stretch) and secondary amine (N-H stretch) were obtained. The absorption range of the hydroxyl group is between 3600–3100 cm^{-1} while the absorption range of secondary amine is 3500–3100 cm^{-1}. Because these two functional groups share almost the same range of wavenumber, the possibility of the overlapping band between them exists [16]. However, the properties between these two functional groups were reported to be related to the –NH stretching vibration [29]. Table 3 presents all the significant wavenumbers of the samples and the corresponding functional group. It can be seen that the wavenumber of –NH stretching vibration of pure Cs is shifted from 3338.78.cm^{-1} to 3325.81 cm^{-1}, 3307.21 cm^{-1}, 3338.40 cm^{-1}, 3325.84.cm^{-1}, and 3272.27 cm^{-1} for Cs-0.4 ml $AgNO_3$, Cs-0.8 ml $AgNO_3$, Cs1.2 ml $AgNO_3$, Cs-1.6 ml $AgNO_3$, and Cs-2.0.ml $AgNO_3$ are respectively. This gradual decreasing pattern in intensity is due to the increase of the silver salt concentrations. The attachment of silver to nitrogen atoms makes the molecules heavier. This is in agreement with Hooke's Law theory explaining the relationship between wavenumber, bond strength, and mass. Therefore, the wavenumber of a bond decreases with the increase of the concentration of the silver salt in the samples.

The main characteristic absorption peaks of pure chitosan and chitosan with different concentrations of silver salt were observed. Only the nitro functional group (N=O stretch) did not present in the pure chitosan making it different from other samples. It is due to that silver nitrate was not added to the pure chitosan sample. Functional groups, like the amine (-NH) group, hydroxyl (-OH) group, and carbonyl (C=O) groups in ketones, aldehydes, and amides were significantly visible. Similar results were found by Aziz et al. [17].

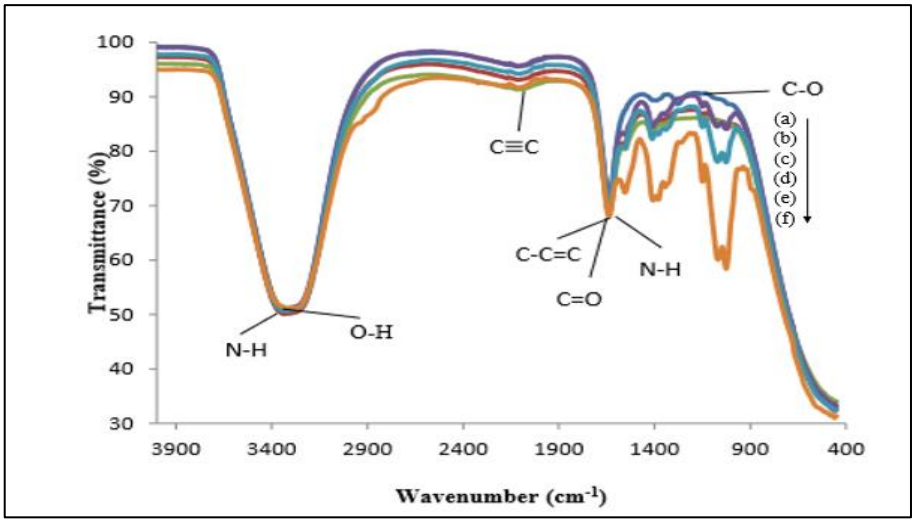

Figure 3. FTIR spectra of (a) Cs-1.2 ml of $AgNO_3$, (b) Cs, (c) Cs-0.4 ml of $AgNO_3$, (d) Cs-0.8 ml of $AgNO_3$, (e) Cs-1.6 ml of $AgNO_3$, (f) Cs-2.0 ml of $AgNO_3$.

The presence of all the functional group's presence in the samples has a role to promote wound-healing processes. For instance, functional groups like $–NH_2$, –NH, and –CO are attributed to improving the cell compatibility and haemocompatibility of the skin [18]. FTIR spectra (Figure 3) illustrate that all the samples are enriched with an amine group. Both primary –NH bend and secondary –NH stretch are exhibited in all the samples. This is the reason that chitosan is also referred to as polymeric amine. Amines play important role in the therapeutic and survival of life. This is due to the contribution of the amine group involved in the creation of amino acid providing protein in human beings.

Moreover, in the context of organic chemistry, amines are important chemicals and basic compounds in biological processes. Furthermore, the amines group is also broadly used in the pharmaceutical industry and developing chemicals for crop protection medication and water purification. Besides the amine group, the hydroxyl (-OH) group also has the properties to fasten wound healing. Chitosan makes an important contribution in the presence of reactive amine and hydroxyl groups. These two functional groups of repeating units make chitosan versatile for chemical modification [19]. Furthermore, the presence of these two groups indicates that wound dressing functions perfectly to transport proteins and other active molecules by physical and chemical means [20]. In addition, the hydroxyl group, regardless of being bonded freely or weakly, can still attract and bond with water. This enhances the ability of wound dressing to absorb exudate. Carbonyl group presence in ketones, aldehydes, and amides results in producing ideal wound dressings. Ketones are famous for their wound-healing properties because of preventing the overproduction of scar tissue and keloid formation, while aldehyde is known as an anti-infectious agent, especially against fungi [21]. The presence of the amide group also contributes to the excellent mechanical and thermal stability of the fibers in wound dressing [22]. In addition, Bolognia et al. (2012) also reported that ketone is always used for wound healing; and a combination of aldehydes and hydroxyl groups has the characteristics of anti-microbial and immunostimulatory properties [23].

Table 3. Functional group of FTIR bands for pure chitosan and chitosan with different concentration of silver nitrate, $AgNO_3$.

Functional group (absorption range) IR vibration	**Wavenumbers (cm^{-1})**					
	Cs	Cs-0.4 ml of $AgNO_3$	Cs-0.8 ml of $AgNO_3$	Cs-1.2 ml of $AgNO_3$	Cs-1.6 ml of $AgNO_3$	Cs-2.0 ml of $AgNO_3$
Alkenes C-C=C Symmetric stretch	1634.89	1635.04	1634.70	1635.27	1635.26	1635.48
Alkynes C≡C stretch	2160.09	2170.92	2161.5	2187.37	2170.65	2188.42
Alcohol O-H stretch	3338.78	3325.81	3307.21	3338.40	3325.84	3272.27
Ketones C=O stretch	1634.89	1635.04	1634.70	1635.27	1635.26	1635.48
Aldehydes C=O stretch	1634.89	1635.04	1634.70	1635.27	1635.26	1635.48
Ethers C-O stretch	1278.43	1150.45	1016.55	1025.89	1026.72	1026.15
Amine – primary N-H bend	1634.89	1635.04	1634.70	1635.27	1635.26	1635.48
Amine – secondary N-H stretch	3338.78	3325.81	3307.21	3338.40	3325.84	3272.27
Nitro N=O stretch	-	1555.35	1553.41	1554.39	1555.10	1554.02
Amides i) C=O stretch ii) N-H bond	1634.89	1635.04	1634.70	1635.27	1635.26	1635.48

Field Emission Scanning Electron Microscope (FESEM) Analysis

FESEM is used to characterize the size of the cell and the size distribution of the samples. FESEM measurement was conducted for all samples to analyze the correlation of surface appearance and surface morphology of the samples. Figure 4 depicts the surface morphology of pure chitosan. It can be seen that the pure chitosan shape morphology resembles a bundle shape. Similar results were found by other researchers using completely different experimental designs and materials. The magnification of pure chitosan is 2300x. Achieving higher magnifications was not possible due to the charging of the sample surface while observing under an electron beam [24].

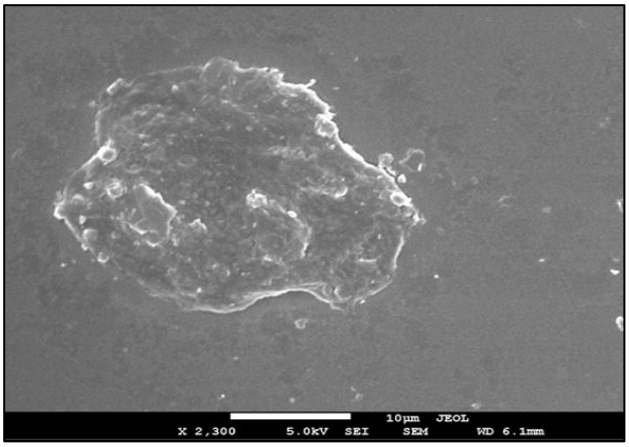

Figure 4. FESEM image of pure chitosan (Cs).

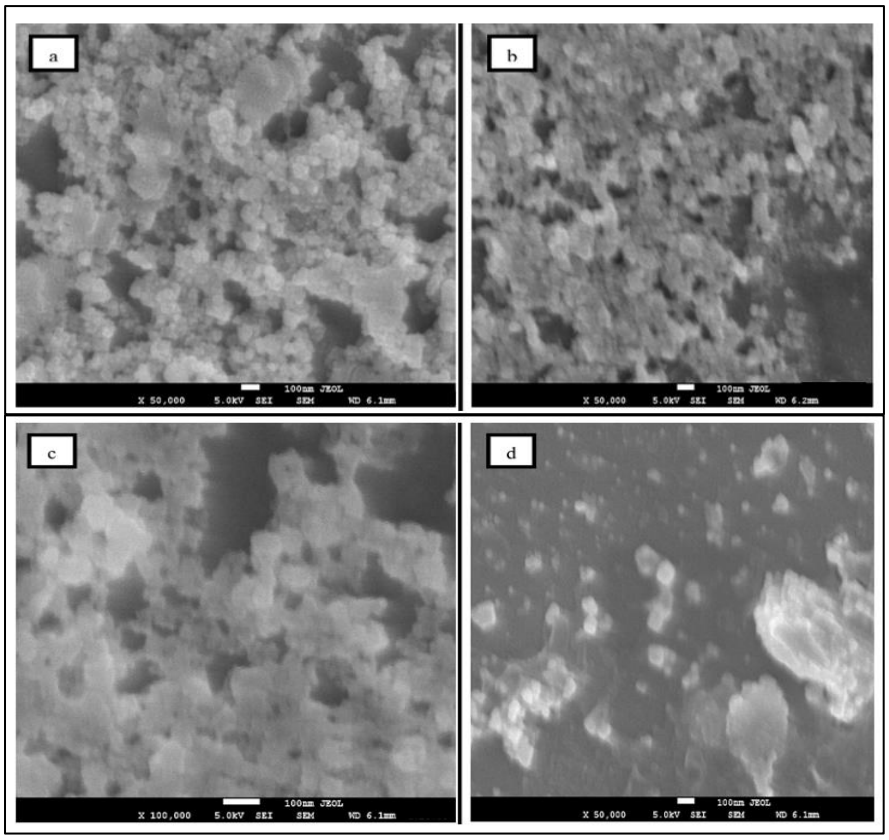

Figure 5. FESEM images of samples (a) Cs & 0.4 ml $AgNO_3$,(b) Cs & 0.8 ml $AgNO_3$,(c) Cs & 1.2 ml $AgNO_3$ and (d) Cs & 1.6 ml $AgNO_3$.

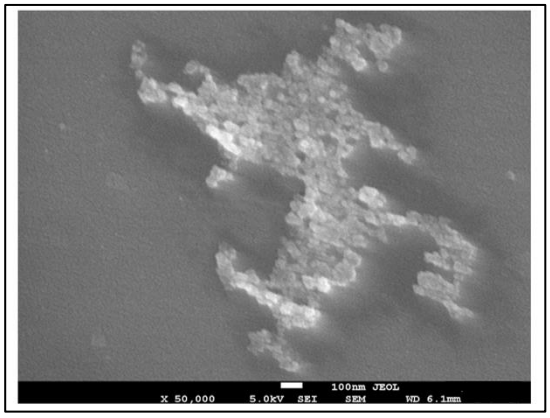

Figure 6. FESEM images of Cs & 2.0.ml $AgNO_3$.

Figure 5 displays the surface morphologies of a combination of chitosan and silver nitrate with different concentrations. The surface morphology of the samples in Figure 5 was in nanoparticles size, according to the definition of nanoparticles as the particles having a range of diameter between 1–100 nm [25]. Surface morphology of Cs-0.4 ml $AgNO_3$, Cs-0.8 ml $AgNO_3$, and Cs-1.2 ml $AgNO_3$ indicate that the shape of particles is almost spherical and plated. Ibrahim et al. (2015) identified a similar morphology for the solution mixture of Cs-AgNPs. In addition, Cs-0.4.ml $AgNO_3$, Cs-0.8 ml $AgNO_3$, and Cs-1.2 ml $AgNO_3$ represent the formation of spherical nanoparticles of silver of the same size. In addition, silver nanoparticles are enveloped by chitosan; and the agglomeration can also be detected [30]. Cs-1.6.ml $AgNO_3$ is the only sample demonstrating proper dispersion of the surface morphology. The agglomeration reduction occurs in chitosan when a higher concentration of silver salt is used. Furthermore, as the agglomeration reduces, the dispersion of silver nanoparticles and the chitosan solution increase. The obtained dispersion and stability in this study are lower than those reported in the previous studies [26] due to the contamination of the sample leading to the introduction of artifacts during sample preparation.

Figure 6 illustrates the surface morphology of Cs-2.0.ml $AgNO_3$. It can be seen that the dispersion and stability are much lower than those of the other samples and also those reported in the previous study [27] due to improper technique during the coating of the glass slide of the sample, hence leading to the deposition problem of the samples. Furthermore, the aggregate formation may result from errors during the sample preparation and storage contributing to the low resolution of the surface morphology.

CONCLUSION

In this study, the non-woven wound dressing was produced from pure chitosan and chitosan loaded with silver nanoparticles with different concentrations of silver nitrate. Based on the obtained results from UV-Vis spectrometer and FTIR spectroscopy, the physical and chemical properties of the treated wound dressing exhibited the potential to fasten the wound healing process due to the presence of functional groups of amine, hydroxyl, and carbonyl in the solution of pure chitosan and chitosan loaded with silver nanoparticles. This study determined the surface morphology of wound dressing solution using FESEM. The sample of Cs-1.6 ml of $AgNO_3$ showed better dispersion than the other samples. Non-woven wound dressing has been used in the medical field for many years. This study provides an optimal environment for wound healing and benefits the industry in producing more economical wound dressings.

ACKNOWLEDGEMENTS

The authors would like to thank the Faculty of Applied Sciences and Technology, Universiti Tun Hussein Onn Malaysia for the facilities provided that make the research possible.

REFERENCES

1. Youbo, D., Qingshan, L. and Zhuang, X. (2012) Antibacterial finishing of Tencel / Cotton nonwoven fabric using Ag nanoparticles-Chitosan composite. *Journal of Engineered Fibers and Fabric*, **7(2)**, 24–29.

2. Ahmed, S. and Ahmad, M. (2015) Chitosan Based Dressings for Wound Care. *Immunochemistry & Immunopathology*, **1(2)**, 1–6.

3. Senel, S. and Clure, S. J. (2004) Potential Applications of Chitosan in Veterinary Medicine. *Advance Drug Delivery Review*, **5**, 1467–1480.

4. Liu, X. F., Guan, Y. L. and Yao, K. D. (2001) Antibacterial action of chitosan and carboxymethylated chitosan. *Journal Applied Polymer Science*, **79**, 1324–1335.

5. Kim, C. H., Choi, J. W., Chun, H. J. and Choi, K. S. (1997) Synthesis of chitosan derivatives with quaternary ammonium salt and their antibacterial activity. *Polymer Bulletin*, **38**, 387–393.

6. Fang, S. W., Li, C. F. and Shih, D. Y. C. (1994) Antifungal activity of chitosan and its preservative effect on low-sugar candied kumquat. *Journal of Food Protection*, **57**,136–140.

7. Wright, J. B., Lam, K., Hanson, D. and Burrell R. E. (1999) Efficacy of topical silver against fungal burn wound pathogens. *American Journal of Infection Control*, **27**, 344–350.

8. Ahamed, M. I. N. and Sastry, T. P. (2011) Wound dressing application of chitosan based bioactive compounds. *International Journal of Pharmacy & Life Sciences*, **2(8)**, 991–996.

9. Dhivya, S., Vijaya, V. and Santhini, E. (2015) Wound dressings – A review. *Biomedicine*, **5(4)**, 24–28.

10. Ariyanchira, S. (2017) Is Malaysian Market Ripe for Advanced Wound Care Products? 3–5.

11. Sood, A., Granick, M. S. and Tomaselli, N. L. (2014) Wound Dressings and Comparative Effectiveness Data. *Adv Wound Care (New Rochelle)*, **3(8)**, 511–529.

12. Regiel, A., Kyzioł, A. and Manuel A. (2013) Chitosan-silver nanocomposites - modern anti-bacterial materials, *CHEMIK*, **(8)**, 688–692.

13. Paulkumar, K., Gnanajobitha, G., Vanaja, M., Pavunraj, M. and Annadurai, G. (2017) Green synthesis of silver nanoparticle and silver based chitosan bionanocomposite using stem extract of Saccharum officinarum and assessment of its anti-bacterial activity. *Advances in Natural Sciences: Nanoscience and Nanotechnology*, **8(3)**, 1–10.

14. Badertscher, M., Bühlmann, P. and Pretsch, E. (2009) Structure Determination of Organic Compounds: Tables of Spectra Data. *Heidelberg: Springer*.

15. Kumar, S. (2008) Organic Chemistry Spectroscopy of Organic Compounds (In proceedings), 1–36.

16. Abdelgawad, A. M., Hudson, S. M. and Rojas, O. J. (2014) Antimicrobial wound dressing nanofiber mats from multicomponent (chitosan / silver-NPs polyvinyl alcohol) systems. *Carbohydrate Polymers*, **100**, 166–178.

17. Aziz, S. B., Abdullah, O. G., Saber, D. R., Rasheed, M. A. and Ahmed, H. M. (2017) Investigation of metallic silver nanoparticles through UV-Vis and optical micrograph techniques. *International Journal of Electrochemical Science*, **12(1)**, 363–373.

18. Gomathi, N., Rajasekar, R., Babu, R. Rajesh, Mishra, Debasish and Neogi, S. (2012) Development of bio/blood compatible polypropylene through low pressure nitrogen plasma surface modification. *Materials Science and Engineering C, Biomimetic Materials, Sensors and Systems*, **32(7)**, 1767–1778.

19. Jiang, T., James, R., Kumbar, S. G. and Laurencin, C. T. (2014) Chitosan as a Biomaterial: Structure, Properties, and Applications in Tissue Engineering and Drug Delivery. *Natural and Synthetic Biomedical Polymers (1st ed.). Elsevier Inc*.

20. Agnihotri, S. A., Mallikarjuna, N. N. and Aminabhavi, T. M. (2004) Recent advances on chitosan-based micro-and nanoparticles in drug delivery. *Journal of Controlled Release*, **100**, 5–28.

21. Bensouilah, J. and Buck, P. (2006) Aroma-dermatology: Aromatherapy in the treatment and care of common skin conditions. *Oxford: Radcliffe Publishing*.

22. Rajendran, S. (2009) Advanced textiles for wound care. *Wood Head Publishing Ltd, CRC press*, 1–175.

23. Bolognia, J., Jorizzo, J. L. & Schaffer, J. V. (2012) Dermatology. Philadelphia: Elsevier Saunders.

24. Jillavenkatesa, A., Dapkunas, S. & Lum, L. -S. H. (2001) Particle size characterization. *Washington: National Institute of Standards and Technology*.

25. Huang, H. A. (2004) Synthesis of chitosan-stabilized gold nanoparticles in the absence/presence of tripolyphosphate. *Biomacromolecules*, **5(6)**, 2340–2346.

26. Liang, D., Lu, Z., Yang, H., Gao, J. and Chen, R. (2016) Article A Novel Asymmetric Wettable AgNPs / Chitosan Wound Dressing: In Vitro and In Evaluation. *ACS Appl Mater Interfaces*, **8(6)**, 3958–3968.

27. Saware, K., Sawle, B., Salimath, B., Jayanthi, K. and Venkataraman, A. (2014) Biosynthesis and Characterization of Silver Nanoparticles Using Ficus Benghalensis Leaf Extract. *International Journal of Research in Engineering and Technology*, **3(05)**, 867–874.

28. Yasir Anwar, Mazhar Ul-Islam, Hani S. H. Mohammed Ali, Ihsan Ullah, Ashi Khalil and Tahseen Kamal (2002) Silver impregnated bacterial cellulose-chitosan composite hydrogels for anti-bacterial and catalytic applications. *Journal of*

Materials Research and Technology, **18**, 2037–2047.

29. Pavan Kumar, D., Mahadevan, R., Digita, P. A., Visnuvinayagam, S., Lekshmi R. G. Kumar, Suseela Mathew, Ravishankar, C. N. and Anandan, R. (2020) Synthesis and biochemical characterization of silver nanoparticles grafted chitosan (Chi-Ag-NPs): in vitro studies on antioxidant and antibacterial applications. *SN Applied Sciences*, **2**, 665.

30. Govindan, S., Nivethaa, E. A. K., Saravanan, R., Narayanan, V. and Stephen A. (2012) Synthesis and characterization of chitosan-silver nanocomposite. *Applied Nanosciences*, **2**, 299–303.